Stress dip under a two-dimensional semipile of grains

I. Zuriguel* and T. Mullin
Manchester Centre for Nonlinear Dynamics, University of Manchester, Manchester, M139PL, United Kingdom

R. Arévalo
Departamento de Física y Matemática Aplicada, Universidad de Navarra, Pamplona, 31008, Spain
(Received 5 October 2007; revised manuscript received 15 January 2008; published 27 June 2008)

The origin of stress dip under the apex of a standard sandpile has stimulated significant debate within the scientific community. On the other hand, it could be argued that a semipile built against a vertical wall is of more practical interest since it serves as a model of dams, dykes, and embankments. There is surprisingly little information available for the stress distribution in this case. Here we show clear experimental evidence that the presence of the wall enhances the dip under a granular pile significantly. Our investigation provides insight into the influence of walls on the orientation of force chains and this appears to be key in enhancing the dip. Moreover, numerical simulations and experiments with different kinds of particles show that the vertical wall induces an alignment of isotropic particles.

DOI: 10.1103/PhysRevE.77.061307 PACS number(s): 45.70.Cc

I. INTRODUCTION

The study of force networks in collections of static granular materials is of considerable interest since their skeletal structures are a vital ingredient of the physics of their load bearing properties [1]. A sandpile provides one of the simplest examples where the distribution of force chains gives insights into the counterintuitive result that the stress distribution at the base of the pile has a minimum below its apex [2–9]. This finding is important since it challenges the assumptions behind isotropic elastic and plastic models used to describe the mechanical properties of granular solids [10].

Models such as the random contact lattice "q model" [11,12] and the oriented force " fixed principal axes (FPA) model" [4,13–15] provide useful descriptions of observations but a consensus on an appropriate theoretical framework has yet to emerge. An assumption of the FPA model is that avalanching during the construction of a pile will induce a directional structure in the stress distribution. Thus the load is directed toward the sides of the pile in a "tentlike" manner [16]. This has been tested experimentally in both three- [5] and two-dimensional piles where the creation history [6,17] and the effects of particle shape [8,9] have been shown to be important. A local minimum is found in the stress profile below the apex in all cases when piles are built by pouring material from a localized source and it is considerably enhanced when elongated particles are used. The properties of granular materials are also known to depend on the degree of order in the arrangement [18–20], size segregation effects [21], particle shape [22], horizontal compressive forces [21,23], and interparticle friction [24,25].

While the sandpile is of significant scientific interest, in practical applications, such as silos, dams, and embankments, the effects of retaining walls are likely to be very important [26]. There are surprisingly few results on a semipile built against a vertical wall [27], and the presence or otherwise of a stress dip is unclear. Here, we investigate the effects of a vertical wall on the properties of the stress transmission in two-dimensional semipiles of disks and elliptical cylinders. Definite enhancement of the dip is found for both types of particles and we use measures of the distributions of primary and secondary chains to gain insight into possible mechanisms behind this. We also provide results which highlight local alignment of the disks by the vertical wall. This appears to be a robust effect since it was present when particles with very different frictional properties were used in experiments and it was also found in numerical simulations where different protocols were used to build the semipile.

II. EXPERIMENTAL SETUP

Details of the experimental apparatus can be found elsewhere [8,9]. The piles were built using the localized source procedure by pouring grains from a hopper with a 7-cm-wide outlet located 57 cm above the base. A vertical copper wall of dimensions 27.5 cm high, 9.5 mm long and 7.0 mm wide was positioned below the center of the hopper outlet. Hence two semipiles were formed in each experimental run and a section of one sample is shown in Fig. 1. The semipiles were found to be statistically independent and we combine all the results as if for a single semipile in an "⌞" boundary. The birefringent particle technique [28] was used to visualize the force chains using back illumination and viewing through a pair of cross polars. Force chains appeared as bright lines and suitable calibration [9] was used to obtain estimates of the vertical stress distributions. The structural properties of the force chain network were analyzed in a piecewise manner and at the smallest scale a chain was defined to be the approximately straight bright region between two consecutive splits [8]. Once all the chains within a pile were isolated, distributions of their angular directions were formed. In addition, distributions of the orientation of the elliptical cylinders were calculated. For both measurements averages were performed over 500 semipiles so that statistically significant results were obtained.

*Also at Departamento de Física y Matemática Aplicada, Universidad de Navarra, Pamplona, E-31008, Spain; iker@fisica.unav.es

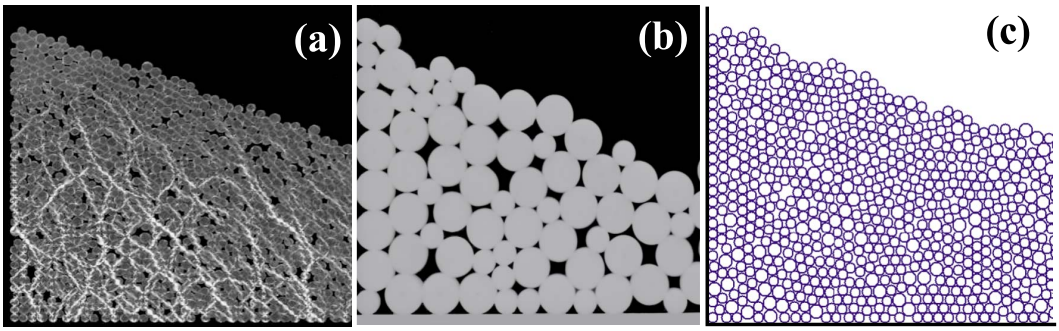

FIG. 1. (Color online) (a) An example of a semipile of disks built near a vertical wall. The disks were poured in a localized way from a 7-cm-wide hopper at 57 cm above the base. (b) Semipile obtained using a mixture of 9 and 6 mm PTFE disks. (c) Semipile obtained using soft particle molecular dynamics simulations of disks in two dimensions with rolling friction and following a protocol similar to the experimental one.

The two types of particles used were 2500 disks with a diameter of 6.9 mm and 500 disks with a diameter of 8.9 mm, and a sample of anisotropic particles which consisted of 2900 elliptic cylinders with dimensions of 9.9 mm and 4.9 mm on the major and minor axes. The thickness of all the particles was 6.6 ± 0.1 mm. In all cases, the polydispersity of the particles was less than 2%. The average angle of repose found for 500 semipiles was $27 \pm 1°$ for the mixture of disks and $36 \pm 1°$ for the elliptic cylinders. The semipiles of disks had an average height of 28 cm and a base length of 56 cm whereas the semipiles of elliptic cylinders had a height of 32 cm and a base length of 44 cm. The packing fraction was 0.82 ± 0.1, which is just below the random close-packed limit of 0.84 in two dimensions (2D) [29].

III. STRESS DIP

The results shown in Fig. 2(a) are estimates of the average vertical stress profiles for semipiles of disks measured at different heights above the base. The main effect is that the dip is considerably enhanced with respect to full piles built using the same procedure [8] so that the presence of a vertical boundary acts to enhance the stress dip. Quantitative estimates of the sizes of the dips can be made by measuring the difference between a Gaussian fit to stress profiles and the data [9]. The amplitude of the dip for a semipile at $h = 3.5$ cm is twice that for a full pile and the area of the dip is ~ 4.5 times larger.

As in the case of full piles [8], semipiles constructed using elliptic cylinders have generally larger dips as shown in Fig. 2(b). The amplitudes are approximately the same for piles and semipiles but the area of the dip is ~ 1.4 times larger for semipiles. Careful inspection of the stress profiles for semipiles of both disks and elliptic cylinders suggests that the stress minimum is displaced from the wall by a thin layer, whereas it is central in full piles.

In order to compare the stress profiles at different heights the results shown in Figs. 2(a) and 2(b) have been rescaled

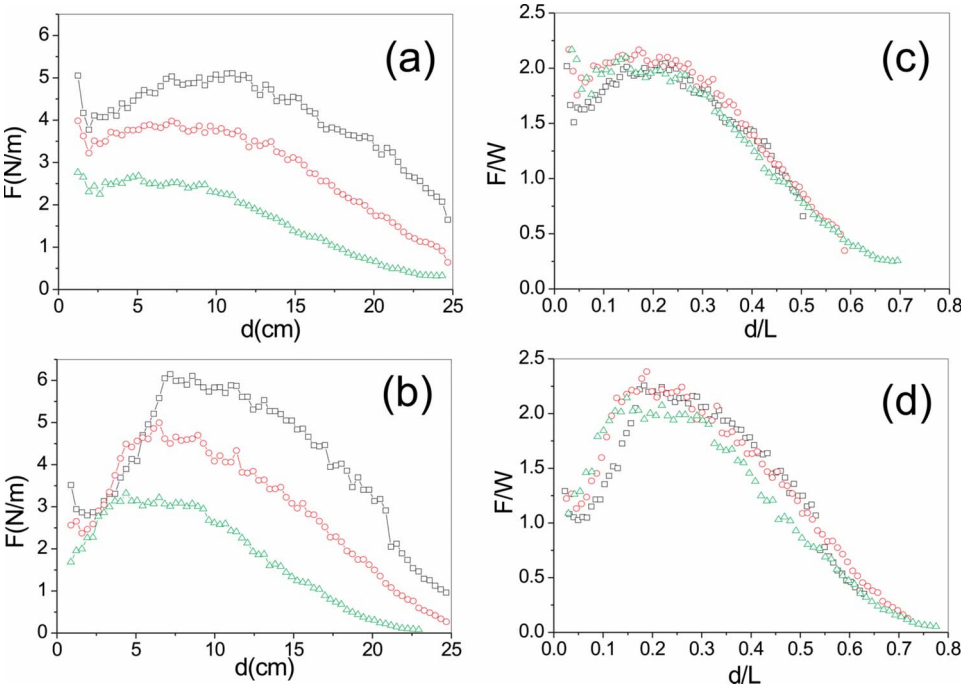

FIG. 2. (Color online) Vertical stress distributions estimated from averaging the results of 500 piles of (a) disks and (b) elliptical cylinders with a boundary placed at $d = 0$. Horizontal slices were taken at $h = 3.5$ cm (□), $h = 7.0$ cm (◯), and $h = 10.5$ cm (△) above the base. Stress distributions normalized with the weight of the particles above each horizontal slice for semipiles of (c) disks and (d) elliptical cylinders.

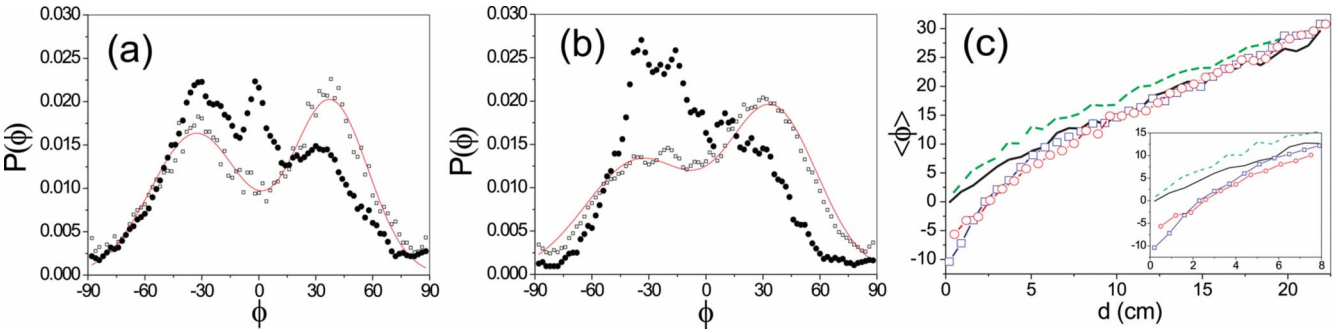

FIG. 3. (Color online) Distribution of the chain orientations found in 500 piles averaged over a 1.5-cm-wide slice centered at $d=2$ cm for (a) semipiles (■) and full piles of disks (□), and (b) semipiles (●) and full piles of elliptic cylinders (□). The solid lines are least-squares fits with bimodal distributions obtained for full piles. (c) Mean chain orientation plotted as a function of distance along the pile. ◯ and □ represent $\langle\phi\rangle$ for semipiles of disks and elliptic cylinders, respectively. The solid and dashed lines correspond to experimental results for $\langle\phi\rangle$ obtained from full piles of disks and elliptic cylinders. Inset: Zoom in of the region near the wall.

by the weight of the granular layer above the height at which each profile has been measured. These results are presented in Figs. 2(c) and 2(d) for disks and elliptical cylinders, respectively. In the case of disks the collapse of the data is good whereas for piles of elliptical cylinders there is a slight dependence of the stress profile on height. Specifically, the lower profiles display a bigger ratio between the width of the dip and that of the pile.

IV. STRESS NETWORKS

The stress networks were analyzed using the angular orientation of the chains, defined as the angle that a chain makes with respect to the normal to the base. For $d>7.0$ cm, the chain orientation distributions obtained from semipiles were indistinguishable from those for the same locations in full piles. However, differences became apparent when comparisons were made using distributions taken from a region near the wall with those near the center of full piles. This effect of the boundary in the chain network is displayed in Figs. 3 where the orientation of the chains that fall in a 1.5 cm width slice centered at $d=2$ cm are presented for full and semipiles of disks [Fig. 3(a)] and full and semipiles of elliptic cylinders [Fig. 3(b)].

In full piles [□ symbols in Figs. 3(a) and 3(b)], the distributions are bimodal with peaks at $\phi=\pm 35$ corresponding to primary and secondary chains. The relative magnitude of the peaks indicate the importance of avalanche alignment (primary chains: $\phi=+35$) over stabilizing effects (secondary chains: $\phi=-35$) across the pile. There are smaller numbers of secondary chains for elliptic cylinders, which were attributed to particle shape induced stability [8,9]. In semipiles [● symbols in Figs. 3(a) and 3(b)], the distributions present a clear inversion of the preferred orientation of the chains for both disks and elliptical cylinders, indicating that the chains are bent toward the wall.

A measure which can be used to characterize the chain structure is the average orientation of the chains $\langle\phi\rangle$ [9]. In Fig. 3(c) the results for the mean chain orientation are plotted as a function of d for full and semipiles of disks and elliptic cylinders. The average orientation of the chains for the right side of a full pile is positive for both disks and elliptic cylinders. On the other hand, for semipiles, $\langle\phi\rangle$ is negative at small distances from the wall ($d<2$ cm). This is a consequence of the fact that the chain orientation distribution near the wall displays the primary peak at $\phi=-35$ [Figs. 3(a) and 3(b)]. This result is important as it proves the bending of chains toward the wall.

The center of the dip in the stress profile for full piles is located at $d=0$ where the transition from positive to negative values of $\langle\phi\rangle$ occurs [9]. Hence, for semipiles, the center of the dip is expected at $d\approx 2$ cm, which is in good agreement with the data obtained for the stress profiles within the pile as in Fig. 2(a). Moreover, a qualitative correlation between the size of the dip and the slope of $\langle\phi\rangle$ versus d at $\langle\phi\rangle=0$ was also found for full piles [9]. In the inset of Fig. 3(c) it can be seen that the slope is greater for semipiles, which is in accord with the increased dip for these cases. An alternative way of considering this result is a natural consequence of the Janssen effect [30]. Frictional interaction with the boundary means that a proportion of the weight is supported by the wall and hence, the chains close to the boundary are oriented toward it.

V. COLUMNAL PARTICLE ARRANGEMENT

An additional effect of the wall on the orientation of the chains is that a significant peak appears at $\phi=0$ when the region close to the wall is analyzed, as shown in Fig. 3(a). This result, which is particularly evident in the case of disks, can be understood from the packing enforced close to the walls. This can be seen in the experimental image presented in Fig. 1(a) and similar wall effects have been reported previously in silos [26]. In order to test the robustness of this effect we conducted a simple illustration experiment using disks with a very low friction coefficient. The sample was a 2:1 mixture of 80 polytetrafluorethylene (PTFE) cylinders with 9 and 5 mm diameters which were 7 mm thick. The container was a plexiglass box $170\times 170\times 8$ mm. An indication of the effects of the low coefficient of friction was that it was not possible to construct a full pile when the box was vertical. We could, of course, artificially construct a pile by

adding one particle at a time when the box was laid flat. However, raising the box very slowly caused this pile to collapse when the box was angled above $\approx 45°$ to the horizontal. Hence, frictional effects from the back and front walls of the box were insufficient to induce stability. By way of contrast, we could use this method to construct a semipile when the box was returned carefully to the vertical position. This provides a simple illustration of the important effect the central boundary has on the stability of a semipile. An example of a semipile constructed using this method is given in Fig. 1(b), where the packing of the particles adjacent to the wall seems to be hexagonal with forced vertical contacts in columns.

In order to further investigate the effect of the wall in the packing of particles, we carried out numerical simulations, and an example of a section of a semipile is given in Fig. 1(c). The numerical results were obtained by the soft particle molecular dynamics method [31]. The model of contact includes a linear restoring force in the normal direction of the impact and a tangential force providing static friction [32]. There is a dissipative term in each direction proportional to the relative respective normal or tangential velocity of the disks. The parameters of the model were given the following values: elastic constant $K_n = 10^5$, dissipative coefficient $\gamma_n = 150$, the corresponding ones in the tangential direction $K_s = \frac{2}{7}k_n$ and $\gamma_s = 300$; frictional coefficient $\mu = 0.5$. The integration time step was set to $10^{-4}\tau$. The stiffness constants k are measured in units of mg/d, the damping constants γ in $m/\sqrt{g/d}$, and time in $\sqrt{d/g}$. Here m, d, and g stand, respectively, for the mass and diameter of the disks and the acceleration of gravity. This model has been used previously to reproduce the flow rate in a silo discharge and good agreement was obtained with experimental results [33]. In the simulations, results are obtained with and without the inclusion of a rolling friction term that introduces a resistance during the relative rotation of two disks in contact [34–36].

The numerical semipiles were constructed using three different construction protocols. The first is equivalent to the experiment as the disks were dropped from a hopper of $6d$ diameter placed $56d$ above the base and there were no lateral side walls. The vertical wall was $2d$ wide and $28.5d$ high and it was located immediately below the exit of the hopper. All the walls were flat with the same properties of stiffness and friction as the grains. The other two protocols were initiated by filling a $40d$ wide box letting a $10d$ wide column of disks fall from a height of $50d$. Once the disks came to rest, one protocol consisted of removing a lateral wall and the subsequent avalanche produced a semipile. The other method involved rotating the box 90° and a semipile was formed as before.

The total number of runs for each protocol was 100 using 2000 disks, 15% with diameter d and 85% with diameter $7/9d$. The comparison of the results of numerical simulations for the distributions of particle contacts (φ) near the wall in a semipile and near the center of a full pile are given in Fig. 4. The results did not depend on the protocol used to build the semipiles and we have chosen to present those obtained with the method closest to the experiment. In all cases the distribution of contacts near the wall has a peak at $\varphi = 0$ indicating a set of vertical contacts.

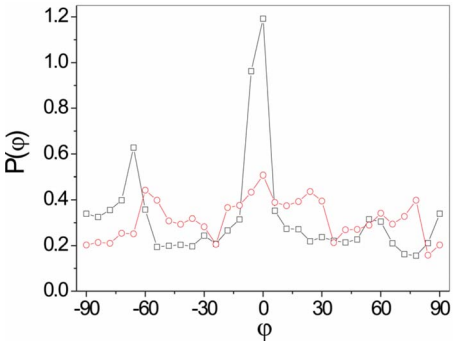

FIG. 4. (Color online) Orientation of particle contacts obtained from numerical simulations in a 1.5-cm-wide slice centered at $d = 2$ cm for semipiles (□) and full piles of disks (◯). These results correspond to numerical simulations carried out with rolling friction and a construction protocol similar to the one used in the experiments.

There is a clear difference between the orientation of particle contacts obtained numerically (Fig. 4) and the orientation of chains near the wall [Fig. 3(b)]. There are several possible reasons for this. The main one is that the orientation of the contacts depends on the normal forces, whereas the orientation of the force chains depends on both the normal and tangential forces. In a previous publication [8], a correlation was found between the orientation of contacts (with a peak at 30°) and the orientation of chains (with a peak at 35°) for disks. However, the magnitudes of the peaks are different and the angular distributions are therefore not the same. Another possible explanation for the difference between the orientation of particle contacts and chains near the wall is related to the photoelastic method, which is only sensitive to forces above 0.5 N m^{-1} [9]. Hence, the distributions of the orientations of chains are only for those chains that carry forces above this value, i.e., contributions from chains carrying small forces are ignored. Indeed, it has been shown by Radjai *et al.* [37,38] that contact forces between grains with magnitudes larger than the average exhibit different properties than smaller ones.

VI. ORIENTATION OF ELLIPTICAL CYLINDERS

Another interesting effect of the boundary is in its influence on the orientation of elliptic particles. In Fig. 5 experimental results are presented for the orientation of elliptical cylinders that fall in a 1.5-cm-width slice centered at $d = 2$ cm for full and semipiles. It is evident that the number of elliptic cylinders oriented vertically is considerably increased by the presence of the vertical wall when compared with data from the center of a full pile. In the latter case, 8.7% of the elliptic cylinders are oriented with angles between $\pm 20°$, whereas this increases to 14.3% close to the wall, and yet the construction process is approximately the same. The orientation of the particles induced by the vertical wall is a short range effect since there were no significant differences between the orientations for full and semipiles in slices taken at $d = 5$ cm from the center and the vertical wall, respectively.

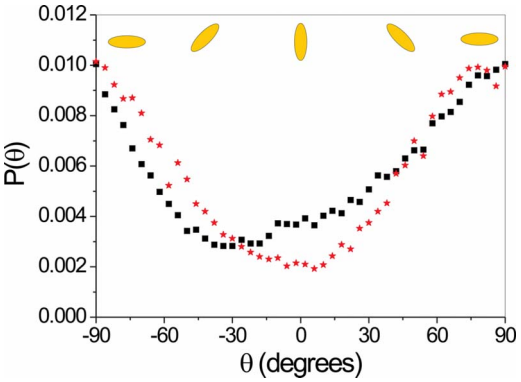

FIG. 5. (Color online) Orientation of the elliptical cylinders that fall in a 1.5 cm width slice centered at $d=2$ cm. (N.B. $d=0$ corresponds to the center of a full pile or the location of the wall for semipiles.) ■ and ⋆ show the results obtained for semipiles and full piles, respectively.

VII. CONCLUSIONS

We have provided clear evidence for the influence of a boundary in the stress transmission within a pile of grains. The dip in the stress is considerably enhanced by the wall and the effect is clearest when disks are used. Analysis of the orientation of the force chains has revealed that the boundary induces an inversion of the chain orientation in its proximities for both anisotropic and isotropic particles. It is this feature that seems to be at the heart of the enhancement of the dip. Additionally, it has been shown that there is a clear preference for columnar packing of disks adjacent to the wall and this seems to have a significant influence on the force distribution [26]. This appears to be a robust effect since it is a feature of observations with both high and low frictional particles and is present in the numerical results obtained for different pile construction protocols. Our data provides a challenge to models and numerical simulations, which thus far have not found evidence for dips in semipiles. We also conclude that stress dips are of direct relevance to a wide range of practical situations and knowledge of the force chain distribution is central to advance our understanding of these issues.

ACKNOWLEDGMENTS

The work of I.Z. was funded by EPSRC by Grant No. GR/T23541/01 and the work of T.M. was also funded by EPSRC. I.Z. also acknowledges partial support from Project No. FIS2005-03881 (MEC, Spain) and PIUNA (University of Navarra). The authors are grateful to J.M. Rotter for helpful discussions concerning these results and to a referee for insisting that we scale the stress profile data.

[1] A. P. F. Atman, P. Brunet, J. Geng, G. Reydellet, P. Claudin, R. P. Behringer, and E. Clément, Eur. Phys. J. E **17**, 93 (2005); S. Ostojic, E. Somfar, and B. Nienhuis, Nature **439**, 828 (2006); J. Zhou, S. Long, Q. Wang, and A. D. Dinsmore, Science **312**, 1631 (2006); F. Radjai, S. Roux, and J. J. Moreau, Chaos **9**, 544 (1999).
[2] T. Jotaki and R. Moriyama, J. Soc. Powder Technol. Jpn. **60**, 184 (1979); J. Smid and J. Novosad, Inst. Chem. Eng. Symp. Ser. **63**, D3/V/1 (1981).
[3] B. Brockbank, J. M. Huntley, and R. C. Ball, J. Phys. II **7**, 1521 (1997).
[4] A. P. F. Atman, P. Brunet, J. Geng, G. Reydellet, P. Claudin, R. P. Behringer, and E. Clément, Eur. Phys. J. E **17**, 93 (2005).
[5] L. Vanel, D. W. Howell, D. Clark, R. P. Behringer, and E. Clément, Phys. Rev. E **60**, R5040 (1999).
[6] J. Geng, E. Longhi, R. P. Behringer, and D. W. Howell, Phys. Rev. E **64**, 060301(R) (2001).
[7] W. McBride, Part. Sci. Technol. **24**, 59 (2006).
[8] I. Zuriguel, T. Mullin, and J. M. Rotter, Phys. Rev. Lett. **98**, 028001 (2007).
[9] I. Zuriguel and T. Mullin, Proc. R. Soc. London, Ser. A **464**, 99 (2008).
[10] K. Terzaghi, *Theoretical Soil Mechanics* (Wiley, New York, 1943).
[11] C.-h. Liu, S. R. Nagel, D. A. Schecter, S. N. Coppersmith, S. Majumdar, O. Narayan, and T. Witten, Science **269**, 513 (1995).
[12] S. N. Coppersmith, C.-h. Liu, S. Majumdar, O. Narayan, and T. A. Witten, Phys. Rev. E **53**, 4673 (1996).
[13] M. E. Cates, J. P. Wittmer, J.-P. Bouchaud, and P. Claudin, Philos. Trans. R. Soc. London, Ser. A **356**, 2535 (1998).
[14] J. Wittmer, P. Claudin, M. E. Cates, and J. P. Bouchaud, Nature (London) **382**, 336 (1996).
[15] J. P. Bouchaud, M. E. Cates, and P. Claudin, J. Phys. I **5**, 639 (1995).
[16] S. F. Edwards and R. B. S. Oakeshott, Physica D **38**, 88 (1989).
[17] J. Geng, E. Longhi, E. Clément, and R. P. Behringer, Physica D **182**, 274 (2003).
[18] M. Da Silva and J. Rajchenbach, Nature (London) **406**, 708 (2000).
[19] J. H. Snoeijer, T. J. H. Vlugt, M. van Hecke, and W. van Saarloos, Phys. Rev. Lett. **92**, 054302 (2004).
[20] L. Breton, P. Claudin, E. Clément, and J.-D. Zucker, Europhys. Lett. **60**, 813 (2002).
[21] K. Liffman, D. Y. C. Chan, and B. D. Hughes, Powder Technol. **78**, 263 (1994); K. Liffman, M. Nguyen, G. Metcalfe, and P. Cleary, Granular Matter **3**, 165 (2001).
[22] H. G. Matuttis, Granular Matter **1**, 83 (1998); H. G. Matuttis, S. Luding, and H. J. Herrmann, Powder Technol. **109**, 278 (2000).
[23] J. Hemmingsson, H. J. Herrman, and S. Roux, J. Phys. I **7**, 291 (1997).
[24] S. Luding, Phys. Rev. E **55**, 4720 (1997).
[25] C. Goldenberg and I. Goldhirsch, Nature (London) **435**, 188 (2005).
[26] I. Bartos and I. M. Janosi, Granular Matter **9**, 81 (2007).
[27] Y. J. Li, Y. Xu, and C. Thornton, Powder Technol. **160**, 219 (2005).
[28] D. W. Howell, R. P. Behringer, and C. T. Veje, Phys. Rev. Lett.

82, 5241 (1999); C. T. Veje, D. W. Howell, and R. P. Behringer, Phys. Rev. E **59**, 739 (1999); T. S. Majmudar and R. P. Behringer, Nature (London) **435**, 1079 (2005).
[29] N. Xu, J. Blawzdziewicz, and C. S. O'Hern, Phys. Rev. E **71**, 061306 (2005).
[30] H. A. Janssen and Z. Ver, Z. Ver. Dtsch. Ing. **39**, 1045 (1895).
[31] J. Schäfer, S. Dippel, and D. E. Wolf, J. Phys. I **6**, 5 (1996).
[32] R. Arévalo, D. Maza, and L. A. Pugnaloni, Phys. Rev. E **74**, 021303 (2006).
[33] C. Mankoc, A. Janda, R. Arévalo, J. M. Pastor, I. Zuriguel, A. Garcimartín, and D. Maza, Granular Matter **9**, 407 (2007).
[34] D. Tabor, Philos. Mag. **43**, 1055 (1952).
[35] F. P. Beer and E. R. Johnson, *Mechanics for Engineers—Statics and Dynamics* (McGraw-Hill, New York, 1976).
[36] Y. C. Zhou, B. D. Wright, R. Y. Yang, B. H. Xu, and A. B. Yu, Physica A **269**, 536 (1999).
[37] F. Radjai, M. Jean, J.-J. Moreau, and S. Roux, Phys. Rev. Lett. **77**, 274 (1996).
[38] F. Radjai, D. E. Wolf, M. Jean, and J.-J. Moreau, Phys. Rev. Lett. **80**, 61 (1998).